

Electronic Supplementary Information for  
**Carbon Nitride Supported AgPd Alloy Nanocatalysts for  
Dehydrogenation of Formic Acid under Visible Light**

Liping Xiao,<sup>a,b</sup> Young-Si Jun,<sup>b,c</sup> Binghui Wu,<sup>b,d,\*</sup> Deyu Liu,<sup>b</sup> Tracy T Chuong,<sup>b</sup> Jie Fan,<sup>a,\*</sup>  
and Galen D. Stucky<sup>b,c,\*</sup>

<sup>a</sup>Department of Chemistry, Zhejiang University, Hangzhou 310027, China

<sup>b</sup>Department of Chemistry & Biochemistry, University of California Santa Barbara, Santa Barbara, CA 93106, United States

<sup>c</sup>School of applied chemical engineering, Chonnam National University, 77 Yongbong-ro, Buk-gu, Gwangju 500-757, Korea

<sup>d</sup> Collaborative Innovation Center of Chemistry for Energy Materials, Xiamen University, Xiamen 361005, China

\*E-mails: bwu@chem.ucsb.edu; jfan@zju.edu.cn; stucky@chem.ucsb.edu

#### EXPERIMENTAL SECTION

**Chemicals.** AgNO<sub>3</sub> (99.9%), formic acid (FA, 88%, 1.22 g/cm<sup>3</sup>), sodium formate (NaCOOH, 99.1%), and Na<sub>2</sub>SO<sub>4</sub> (99.9%) were purchased from Fisher Scientific; K<sub>2</sub>PdCl<sub>4</sub> (99%) from Strem Chemicals; melamine (99%), dimethyl sulfoxide (DMSO, ≥99.5%), Pluronic<sup>®</sup> P123 (Poly(ethylene glycol)-block-poly(propylene glycol)-block-poly(ethylene glycol) (average Mn≈5,800), polyvinylpyrrolidone (PVP, average Mw≈55,000), palladium on carbon (Pd/C, 10 wt% loading), and fumed silica (SiO<sub>2</sub>, 99.8%) from Sigma-Aldrich; cyanuric acid (99%) from Alfa Aesar. Argon (Ar, 99.999%) and nitrogen (N<sub>2</sub>, 99.999%) were purchased from Praxair. All chemicals were used as received without further purification.

**Synthesis of graphitic CN.** CN was prepared according to our previously reported method.<sup>S1</sup> Microsized mesoporous carbon nitride hollow spheres were synthesized by using 1:1 hydrogen-bonded melamine-cyanuric acid network. DMSO was utilized as a solvent to dissolve melamine and cyanuric acid, because of their limited solubility in normal solvent. In a typical synthesis, 0.5 g of melamine and 0.51 g of cyanuric acid were dissolved in 20 mL and 10 mL of DMSO, respectively, with sonication. After complete dissolution, both solutions were kept at room temperature and then mixed together for 10 min to give white precipitates. The mixture was then filtered and washed with ethanol. The resulting white powder was dried at 50 °C and calcined at 550 °C for 4 h with heating rate 2.3 °C min<sup>-1</sup> under nitrogen.

**Preparation of CN-supported AgPd catalysts.** In a typical synthesis of 3 wt% AgPd/CN, 97 mg CN was

mixed in 30 mL ultrapure water (18.2 M $\Omega$  Milli Q) and stirred overnight. Then 1.2 mL (20 mM) aqueous P123, 0.71 mL 20 mM aqueous K<sub>2</sub>PdCl<sub>4</sub>, 0.71 mL 20 mM aqueous AgNO<sub>3</sub> were added into the mixture and stirred for another 30 min. 5 mL 0.1 M aqueous ascorbic acid (AA) was added and stirred for 2 hours. The gray mixture was filtered and washed by water several times, and then dried in a vacuum oven at 60 °C overnight.

**Characterization.** TEM (including high-resolution transmission electron microscopy, HRTEM) studies were performed on a TECNAI FEI-20 transmission electron microscope operating at 200 kV or a TECNAI Titan high-resolution transmission electron microscopy operating at 300 kV. The samples were prepared by dropping ethanol/water dispersion of samples onto 200-mesh carbon-coated copper grids and slowly evaporating the solvent. X-ray Powder Diffraction (XRD) measurements were taken on a Panalytical X'pert PRO diffractometer using Cu K $\alpha$  radiation, operating at 45 kV and 40 mA. The samples were prepared by tableting the powder on a glass holder for measurements. All Photoluminescence (PL) spectra were measured by microplate spectrofluorometer (Gemini EM-Molecular Devices, USA). The excitation wavelength is 350 nm. X-ray photoelectron spectroscopy (XPS) data were collected in a Kratos Axis Ultra X-ray Photoelectron Spectroscopy system, using dry samples. UV-vis absorption spectra were measured on a Shimadzu UV3600 instrument equipped with an integrating sphere diffuse reflectance accessory using BaSO<sub>4</sub> as the reference.

**Dehydrogenation of FA.** (Photo)catalytic hydrogen evolution was performed in a quartz bottle with an approximate 50-mL volume. In a typical test, the catalyst powder (20 mg) and 0.78 mL 5 M NaCOOH was dispersed in 8.8 mL ultrapure water. Argon was purged through the cell for 20 min before reaction to remove oxygen. Then 0.4 mL 88% FA was injected into the reactor. The temperature for all the catalytic reactions was kept at 30 °C. An upside-down burette was used to collect the evolved gases and the volume was read from the scale. Gas products were collected at different stages to monitor the volume increase, and the composition was analyzed on gas chromatograph (GC) with a thermal conductivity detector. When performing photocatalysis, a 300 W Xe lamp (Newport Corporation) was used as the light source, and the UV part of the light was removed by a cutoff filter ( $\lambda > 400$  nm).

In all cases of this work, no CO was detected by the same GC analysis (the detection limit for H<sub>2</sub> and CO in GC is 1 ppm). The decreasing catalytic activity mainly comes from the decreasing concentration of FA, which is well demonstrated previously.<sup>S2</sup>

The TOFs are calculated using the initial 15-min data and the total metal number but surface atoms. Since the real-time decreasing concentration of FA would affect the catalytic activity,<sup>S2</sup> it is reasonable to calculate the TOF before the concentration decreased too much. It is common to use the initial TOFs for comparison in the catalytic activity.<sup>S3-9</sup>

When testing the isotope effect, 9.6 mL D<sub>2</sub>O and 0.265 g NaCOOH was added instead of 8.8 mL H<sub>2</sub>O and 0.78 mL 5 M NaCOOH. The gas composition after 1 hr was measured by a home-made mass spectrometer. The initial reaction solution contained 0.532 mol D<sub>2</sub>O, 0.00325 mol H<sub>2</sub>O (from the FA solution), 0.00920 mol HCOOH, and 0.00390 mol NaCOOH. Initially  $[D]/([D]+[H]) = 97.4\%$ .

When testing the photocatalytic stability of AgPd/CN (Figure S6), the catalysts after each test were collected by centrifugation at 8000 rpm for 10 min and then washed by water for 3 times. The solid after centrifugation was then dispersed in 5-mL water, and transferred from centrifugation tubes to the reaction quartz bottle before drying in a vacuum oven at 60 °C for at least 3 hours to dry and re-activate the catalysts. Then 8.8 mL ultrapure water and 0.78 mL 5 M NaCOOH was added into the above quartz bottle containing the dried catalysts. After sonicating, argon was purged through the quartz bottle for 20 min before reaction to remove oxygen. Then 0.4 mL 88% FA was injected into the reactor. The temperature for all the catalytic reactions was kept at 30 °C. An upside-down burette was used to collect the evolved gases and the volume was read from the scale. If needed, gas products were collected at different stages to monitor the volume increase, and the composition was analyzed on gas chromatograph (GC) with a thermal conductivity detector. When performing photocatalysis, a 300 W Xe lamp (Newport Corporation) was used as the light source, and the UV part of the light was removed by a cutoff filter ( $\lambda > 400$  nm).

**Photocurrent measurement.** The photocurrent was conducted on FTO covered by samples as working electrode and measured at -0.9 V (vs. Ag/AgCl) by Bio-Logic VMP3 potentiostat using Pt and Ag/AgCl as counter and reference electrode, respectively. The supporting electrolyte was an aqueous solution of Na<sub>2</sub>SO<sub>4</sub> (0.2 M) with FA (1 M) and purged with nitrogen for 0.5 h before measurement. Pure CN, Pd/CN, or AgPd/CN electrode was prepared by spreading aqueous slurries of catalysts over FTO glass substrate. The suspension was prepared by dispersing 50 mg of catalysts in 2 mL of 1 wt% Nafion in ethanol. The film was annealed at 60 °C for 2 h under air before testing. The working electrode was irradiated from the back. Visible light was generated by a 300 W Xe lamp (Newport Corporation) with a 400 nm cut-off filter and was chopped manually.

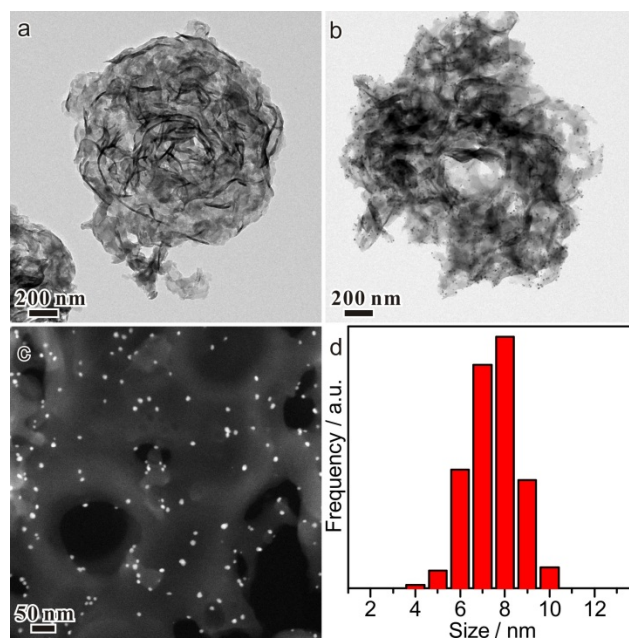


**Figure S1.** (a) TEM image of pure CN. (b) TEM, (c) STEM images, and (d) size distribution of AgPd/CN-3wt%. Average size shown in (d):  $7.5 \pm 1.0$  nm.

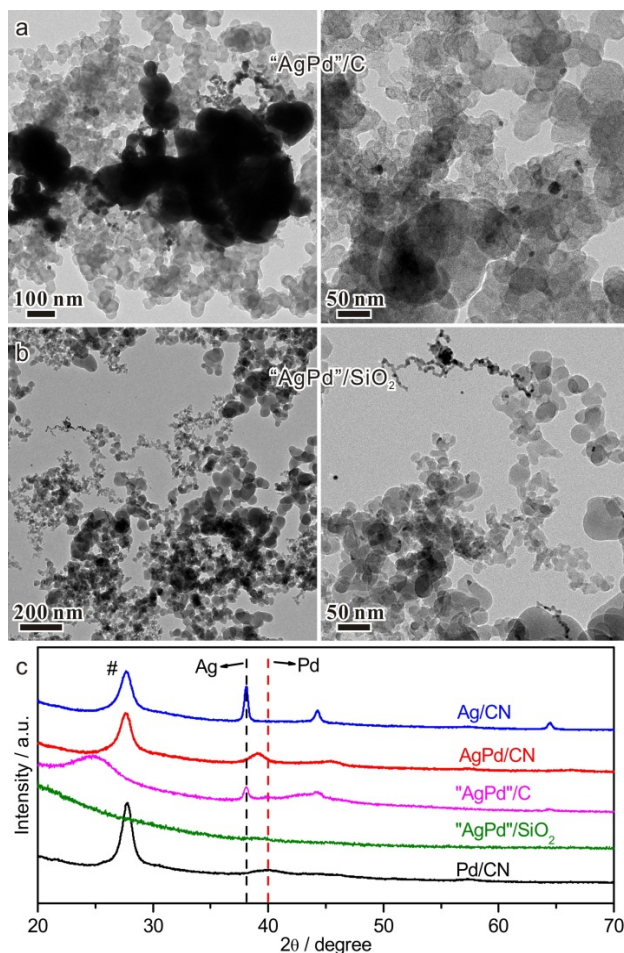


**Figure S2.** Support effect in the synthesis of supported AgPd catalysts with the same feed of precursors in the case of AgPd/CN-3wt% shown in Figures 1 and S1. TEM images of (a) “AgPd”/C synthesized in the presence of activated carbon and (b) “AgPd”/SiO<sub>2</sub> synthesized by in the presence of fumed silica. (c) Comparisons of XRD patterns of three supported AgPd samples. XRD patterns of Ag/CN and Pd/CN (Figure S4) are also shown here for comparison.

“AgPd” means that although Ag and Pd precursors were added and reduced together, the resulting metal nanoparticles might not be an alloy, according to the XRD pattern.

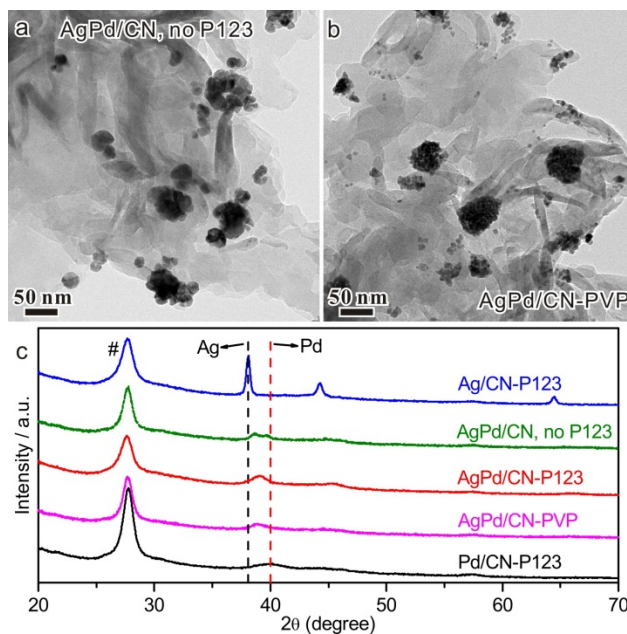


**Figure S3.** Surfactant effect in the synthesis of AgPd (3 wt% metal amount) supported on the same support of CN. TEM images of (a) AgPd/CN synthesized without adding any surfactant and (b) AgPd/CN synthesized by adding PVP instead of P123. (c) Comparisons of XRD patterns of three AgPd/CN samples. XRD patterns of Ag/CN and Pd/CN (Figure S4) are also shown here for comparison.

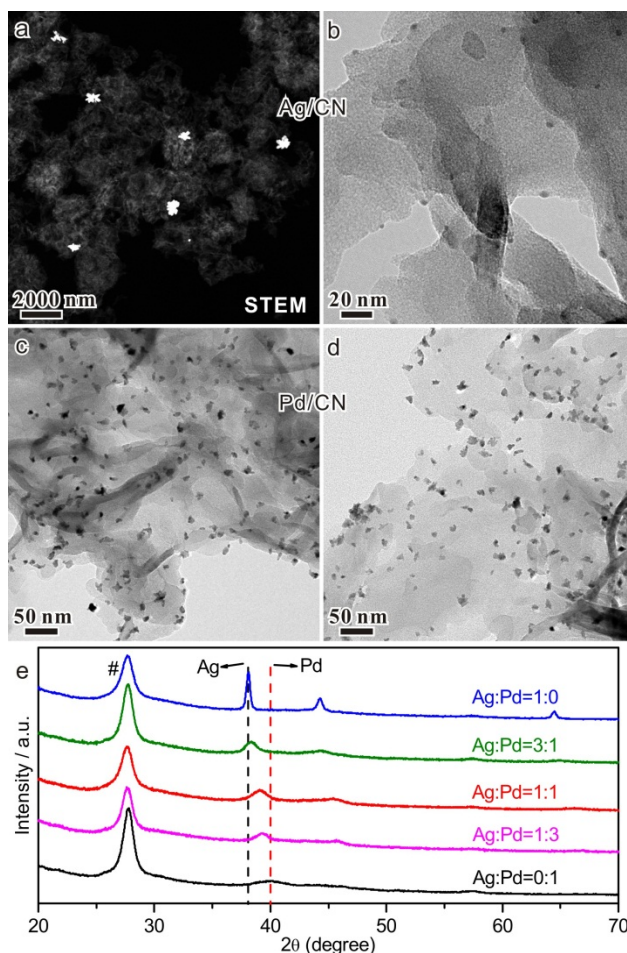


**Figure S4.** Comparison of Ag and Pd (3 wt% metal amount) on CN support. (a) STEM and (b) TEM images of Ag/CN. (c, d) TEM images of Pd/CN. (e) XRD patterns of CN-supported catalysts with different ratio of Ag and Pd. Only large aggregated nanoparticles were obtained in the absence of Pd, assigned to the strong peak intensity in the XRD of Ag/CN.

From Figure S4, both large ( $> 50$  nm) and small ( $\sim 3$  nm) Ag nanoparticles were obtained in the Ag/CN case. However, only small metal nanoparticles were obtained in the Pd/CN and AgPd/CN cases. Also, much higher particle density was found in the Pd/CN and AgPd/CN cases than Ag/CN. We conclude that the significant difference in peak width and intensity (Ag/CN vs others) comes from the difference in particle size.

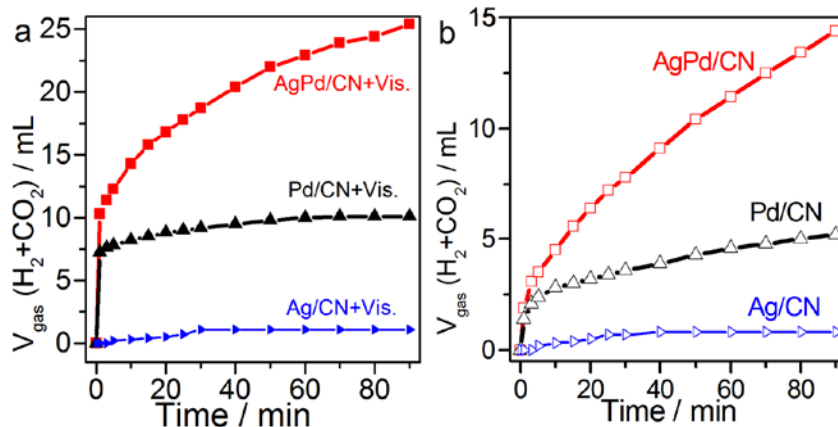


**Figure S5.** Detailed catalytic activity of FA decomposition by AgPd/CN-3%, Ag/CN-3% and Pd/CN-3% at 30 °C with (a) visible light (>400 nm) or (b) under dark. All the gas contained 1:1 (v:v) H<sub>2</sub> and CO<sub>2</sub>, and no detectable CO, confirmed by the same gas chromatography analysis.

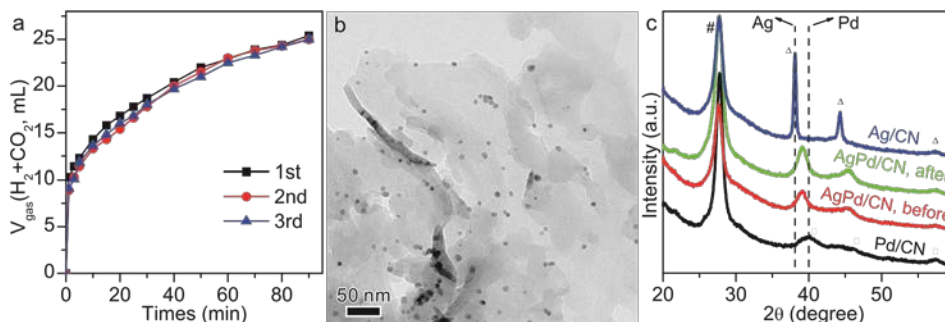


**Figure S6.** (a) Comparison of photocatalytic activity among three repeated tests on the AgPd/CN-3% photocatalysts (see Experimental Section for more details). (b) TEM image of the collected AgPd/CN-3% photocatalysts after 3 cycles under visible light. (c) Comparison of XRD patterns of the AgPd/CN-3% photocatalysts before and after 3 cycles (#, CN;  $\Delta$ , Ag;  $\square$ , Pd).

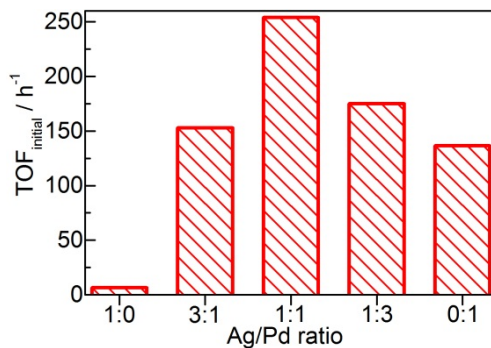


**Figure S7.** Comparison of catalytic activity of FA decomposition under visible light by

CN-supported catalysts with different ratios of Ag and Pd. This reveals that the catalytically active sites in AgPd/CN are Pd, other than Ag or CN. Ag here acts as electron promoter, while CN acts as support.

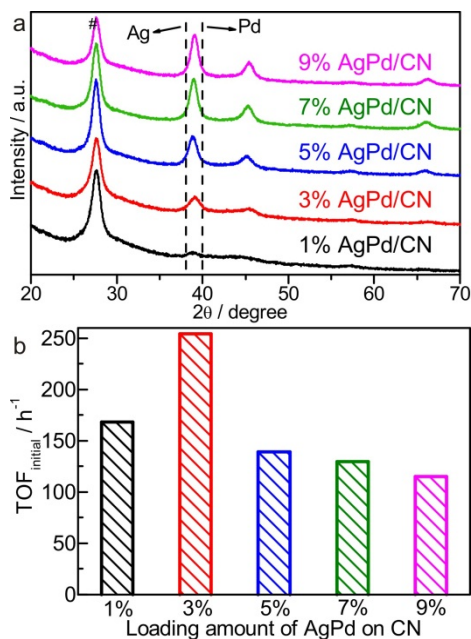


**Figure S8.** Comparison of catalytic activity of FA decomposition under visible light by CN-supported catalysts with different loading amounts of AgPd (1:1): (a) XRD, (b) TOFs of FA decomposition.

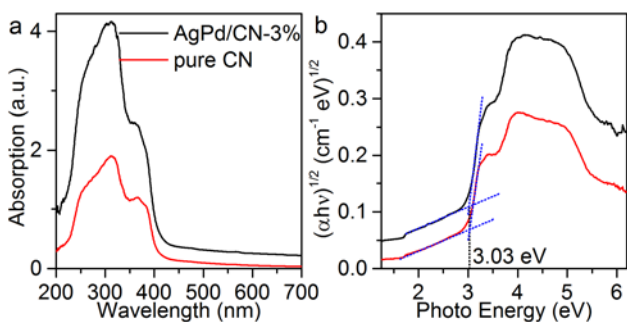


**Figure S9.** (a) Diffuse reflectance UV-vis absorption spectra and (b) corresponding Tauc curves of AgPd/CN-3% and pure CN. They have the same absorption edge (410 nm) and band gap (3.03 eV). Note that the absorption is not completely zero until 700 nm.

## References:

- S1 Y.-S. Jun, E.Z. Lee, X. Wang, W.H. Hong, G.D. Stucky, A. Thomas, *Adv. Funct. Mater.*, 2013, **23**, 3661-3667.
- S2 Y.-Y. Cai, X.-H. Li, Y.-N. Zhang, X. Wei, K.-X. Wang, J.-S. Chen, *Angew. Chem. Int. Ed.*, 2013, **52**, 11822-11825.
- S3 S. Zhang, Ö. Metin, D. Su, S. Sun, *Angew. Chem. Int. Ed.*, 2013, **52**, 3681-3684.
- S4 K. Mori, H. Tanaka, M. Dojo, K. Yoshizawa, H. Yamashita, *Chem.-Eur. J.*, 2015, **21**, 12085-12092.
- S5 C. Hu, X. Mu, J. Fan, H. Ma, X. Zhao, G. Chen, Z. Zhou, N. Zheng, *ChemNanoMat*, 2016, **2**, 28-32.
- S6 J.F. Hull, Y. Himeda, W.-H. Wang, B. Hashiguchi, R. Periana, D.J. Szalda, J.T. Muckerman, E. Fujita, *Nat. Chem.*, 2012, **4**, 383-388.
- S7 Q.-Y. Bi, X.-L. Du, Y.-M. Liu, Y. Cao, H.-Y. He, K.-N. Fan, *J. Am. Chem. Soc.*, 2012, **134**, 8926-8933.
- S8 K. Mori, M. Dojo, H. Yamashita, *ACS Catal.*, 2013, **3**, 1114-1119.
- S9 X. Gu, Z.-H. Lu, H.-L. Jiang, T. Akita, Q. Xu, *J. Am. Chem. Soc.*, 2011, **133**, 11822-11825.